

# The Effects of Moisture on LiD Single Crystals Studied by Temperature Programmed Reaction

*L.N. Dinh, M. Balooch, C.M. Cecala, J.H. Leckey*

This article was submitted to  
23<sup>rd</sup> Aging, Compatibility and Stockpile Stewardship Conference  
Livermore, CA, November 14-16, 2000

**September 14, 2000**

*U.S. Department of Energy*

Lawrence  
Livermore  
National  
Laboratory

## DISCLAIMER

This document was prepared as an account of work sponsored by an agency of the United States Government. Neither the United States Government nor the University of California nor any of their employees, makes any warranty, express or implied, or assumes any legal liability or responsibility for the accuracy, completeness, or usefulness of any information, apparatus, product, or process disclosed, or represents that its use would not infringe privately owned rights. Reference herein to any specific commercial product, process, or service by trade name, trademark, manufacturer, or otherwise, does not necessarily constitute or imply its endorsement, recommendation, or favoring by the United States Government or the University of California. The views and opinions of authors expressed herein do not necessarily state or reflect those of the United States Government or the University of California, and shall not be used for advertising or product endorsement purposes.

This is a preprint of a paper intended for publication in a journal or proceedings. Since changes may be made before publication, this preprint is made available with the understanding that it will not be cited or reproduced without the permission of the author.

This report has been reproduced  
directly from the best available copy.

Available to DOE and DOE contractors from the  
Office of Scientific and Technical Information  
P.O. Box 62, Oak Ridge, TN 37831  
Prices available from (423) 576-8401  
<http://apollo.osti.gov/bridge/>

Available to the public from the  
National Technical Information Service  
U.S. Department of Commerce  
5285 Port Royal Rd.,  
Springfield, VA 22161  
<http://www.ntis.gov/>

OR

Lawrence Livermore National Laboratory  
Technical Information Department's Digital Library  
<http://www.llnl.gov/tid/Library.html>

# **The effects of moisture on LiD single crystals studied by Temperature Programmed Reaction**

**L. N. Dinh, M. Balooch**

Chemistry and Materials Science

Lawrence Livermore National Laboratory, Livermore, CA

**C. M. Cecala, J. H. Leckey**

Lockheed Martin Energy Systems, Oak Ridge, TN

## **ABSTRACT**

Temperature programmed reaction (TPR) technique was performed on LiOH powders and LiD single crystals previously exposed to different moisture levels. Our results show that the LiOH decomposition process has an activation energy barrier of 30 to 33.1 kcal/mol. The LiOH structure is stable even if kept at 320 K for 100 years. However, LiOH structures formed on the surface of LiD during moisture exposure at low dosages may have multiple activation energy barriers, some of which may be much lower than 30 kcal/mol. We attribute the lowering of the activation energy barrier for the LiOH decomposition to the existence of dangling bonds, cracks, and other long range disorders in the LiOH structures formed at low levels of moisture exposure. These defective LiOH structures may decompose significantly over the next 100 years of storage even at room temperature. At high moisture exposure levels, LiOH.H<sub>2</sub>O formation is observed. The release of H<sub>2</sub>O molecules from LiOH.H<sub>2</sub>O structure has small activation energy barriers in the range of 13.8 kcal/mol to 16.0 kcal/mol. The loosely bonded H<sub>2</sub>O molecules in the LiOH.H<sub>2</sub>O structure can be easily pumped away at room temperature in a reasonable amount of time. Our experiments also suggest that handling LiD single crystals at an elevated temperature of 340 K or more reduces the growth rate of LiOH and LiOH.H<sub>2</sub>O significantly. Therefore, a proposed way of minimizing hydrogen formation (due to H<sub>2</sub>O reaction with LiD) in a closed system containing LiOH in the presence of LiD may be to handle LiD at a slightly, elevated temperature during the assembly.

## **I. INTRODUCTION**

As a result of exposure to water vapor during routine handling, a corrosion layer will form on the surface of lithium deuteride. It is believed that depending on the conditions of exposure, LiOH and/or Li<sub>2</sub>O are formed with some LiOH·H<sub>2</sub>O formation at higher exposure levels. In a closed system, LiOH will react with LiD to generate hydrogen gas (H<sub>2</sub>, HD, D<sub>2</sub>). A recent literature review indicates that there are still many unanswered questions concerning the interaction of LiD with H<sub>2</sub>O.<sup>1,2</sup> Several simple models have been proposed to explain some of the observed results of H<sub>2</sub>O exposure.<sup>1-2</sup> However, more detailed studies are needed to obtain insight on the mechanism involved for such a complex reaction system and to handle LiD in different environments. Additionally, it is desirable to determine the kinetic parameters for the reactions resulting from H<sub>2</sub>O exposure in order to model the long-term behavior of LiD in a closed system.

In order to better understand the LiD and H<sub>2</sub>O interaction, temperature programmed reaction (TPR) experiments have been conducted on LiOH powders and LiD single crystals under a variety of environmental conditions. The activation energies have been determined over a range of H<sub>2</sub>O exposure levels.

## **II. EXPERIMENTS**

LiOH powders were prepared by reacting LiD powders in a beaker containing liquid H<sub>2</sub>O over an extended period of time (many days). Water was allowed to evaporate at room temperature, leaving the powders behind. The powders were then wrapped inside a Pt envelope. The side of the envelope facing the mass-spectrometer was perforated with

many holes over the entire surface. The loaded foil was held fixed to a sample holder by way of three mechanical clamps and transferred into an ultrahigh vacuum (UHV) chamber with a base pressure of  $10^{-6}$  Pa ( $4 \times 10^{-7}$  Pa in the detector chamber) through a differentially pumped load lock. The sample was pumped in the UHV chamber for a few hours to remove  $\text{H}_2\text{O}$  molecules that were loosely bonded to the powders. A type K thermocouple was inserted between the Pt envelope surface and a clamp holding the envelope for temperature measurement. The samples were heated by passing currents through a tungsten coil located 2 mm behind the samples. The detector chamber is equipped with a quadrupole mass spectrometer (QMS) and has been described in detail elsewhere.<sup>3</sup>

Some LiD single crystals were cleaved in air, then exposed to ambient air for a certain length of time prior to TPR experiment. Others were cleaved in a glove bag which was attached directly to the entrance port of the TPR load chamber and back-filled with  $\text{N}_2$  (10 to 20 % relative humidity). In a TPR experiment, the cleaved LiD sample was held fixed to a sample holder by way of three mechanical clamps and transferred into the main TPR chamber as mentioned above. The samples, which had been cleaved in the glove bag, were also heat-treated at a predetermined temperature for a given length of time, cooled down to room temperature, then exposed to a studied level of moisture for a planned amount of time. All samples were pumped for some time (a few hours to a few days) prior to TPR experiment.

### III. ANALYSIS TECHNIQUES

#### **The kinetic equations for TPR**

During TPR, LiOH decomposes by the overall reaction:



Conservation of elements implies:

$$-2 \frac{d[\text{LiOH}]}{dt} = \frac{d[\text{H}_2\text{O}]}{dt} \quad (2)$$

Here, [ X ] represents the number of molecules X at time t. The term on the right hand side of equation (2) is, experimentally, the flux of H<sub>2</sub>O detected by the mass spectrometer.

The term on the left of equation (2) represents the reaction rate of LiOH which is twice the experimentally measured rate of production of H<sub>2</sub>O. It is also noted that due to the pumping action of the cryo-pumps in our TPR experiment, H<sub>2</sub>O (g) was continuously pumped out of the system. As a result reaction (1) can be assumed to always go in the forward direction irrespective of the amount of Li<sub>2</sub>O (s) formed.

Let N<sub>H<sub>2</sub>O</sub> be the total amount of H<sub>2</sub>O produced at the end of the TPR run. N<sub>H<sub>2</sub>O</sub> can be obtained experimentally from the TPR spectrum:

$$N_{\text{H}_2\text{O}} = \int_0^{\infty} \frac{d[\text{H}_2\text{O}]}{dt} dt \quad (3a)$$

Let N<sub>LiOH</sub> be the initial amount of LiOH, then from reaction (1):

$$\int_0^{\infty} -\frac{d[\text{LiOH}]}{dt} dt = N_{\text{LiOH}} = \frac{1}{2} N_{\text{H}_2\text{O}} \quad (3b)$$

Observe that:

$$-\frac{1}{N_{LiOH}} \frac{d\{LiOH\}}{dt} = -\frac{d\left\{\frac{[LiOH]}{N_{LiOH}}\right\}}{dt} = \frac{1}{N_{H_2O}} \frac{d[H_2O]}{dt} = \frac{d\left\{\frac{[H_2O]}{N_{H_2O}}\right\}}{dt} \quad (4)$$

$$\text{Let } \mathbf{f} \equiv \left\{ \frac{[LiOH]}{N_{LiOH}} \right\} \quad (5)$$

The reaction rate becomes<sup>4,7</sup>:

$$\text{rate} = \frac{d\left\{\frac{[H_2O]}{N_{H_2O}}\right\}}{dt} = -\frac{d\mathbf{f}}{dt} = k\mathbf{f}^n \quad (6)$$

with

$$k = \mathbf{u} e^{-\frac{E}{RT}} \quad (7)$$

where n is the empirical kinetic reaction order, which may not necessarily be equal to 2 as implied in reaction (1). This is because the formation of H<sub>2</sub>O (g) may not be an elementary process as described in reaction (1), but may consist of many intermediate steps.<sup>4,5</sup>

Employing a linear heating rate  $T = T_0 + \mathbf{b} t$  where  $\beta$  is the ramp rate, equation (6)

becomes:

$$-\frac{d\mathbf{f}}{dT} = \frac{\mathbf{u}}{\mathbf{b}} e^{-\frac{E}{RT}} [\mathbf{f}]^n \quad (8)$$

With some mathematical approximation,<sup>7,8</sup> equation (8) can be rewritten as:

$$-\frac{d\mathbf{f}}{dT} = \frac{\mathbf{u}}{\mathbf{b}} e^{-\frac{E}{RT}} \left[ 1 + (n-1) \frac{\mathbf{u}}{\mathbf{b}} \frac{RT^2}{E} e^{-\frac{E}{RT}} \right]^{\frac{n}{(1-n)}} \text{ for } n \neq 1 \quad (9)$$

and

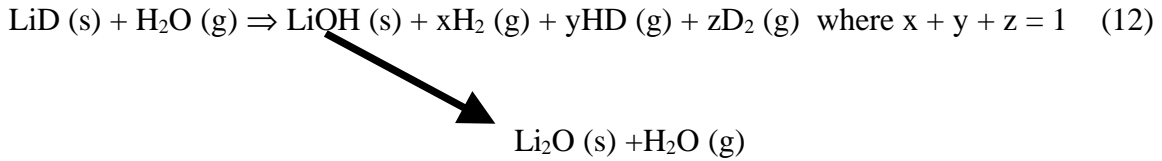
$$-\frac{df}{dT} = \frac{u}{b} \exp\left(-\frac{E}{RT} - \frac{u}{b} \frac{RT^2}{E} e^{-\frac{E}{RT}}\right) \text{ for } n=1 \quad (10)$$

### TPR of LiOH in the presence of LiD

The overall reaction (not listing intermediate processes) is given by:



If there is any residual pocket of LiD remaining in the LiOH powders, the following reactions may accompany:



In TPR experiments, we supply heat to accelerate the decomposition of LiOH into solid Li<sub>2</sub>O and H<sub>2</sub>O molecules which are actively driven off the decomposition site by the pumping action in the TPR chamber. For this reason, only a fraction of the H<sub>2</sub>O molecules generated in the decomposition process (11) will react with LiD in the vicinity according to reaction (12). However, in a closed system where there is no other pump but LiD, many more H<sub>2</sub>O molecules will eventually find their way to the sites with LiD and react according to reaction (12). Hence, in a closed system containing both LiD and LiOH, the end result of the LiOH decomposition process is, therefore, a generation of H<sub>2</sub>, HD, and D<sub>2</sub>.

It is noted that ΔG for reaction (11) is positive in the range < 1000 C while ΔG for reaction (12) is negative in the same temperature range. As long as the diffusion of water through LiOH film is fast, conversion of water to hydrogen according to reaction (12)

should be relatively fast in a closed system. Reaction (11) is, therefore, the rate limiting step.

### Experimental determination of the TPD/TPR kinetic reaction order $n$

Equations (9) and (10) can be used to simulate TPD/TPR curves of different kinetic reaction order  $n$ . Fig.1 shows TPR curves for  $n = 0.75$  and  $n = 0.25$ . Note that as  $n$  gets closer to 0, the TPR curve becomes more asymmetric.

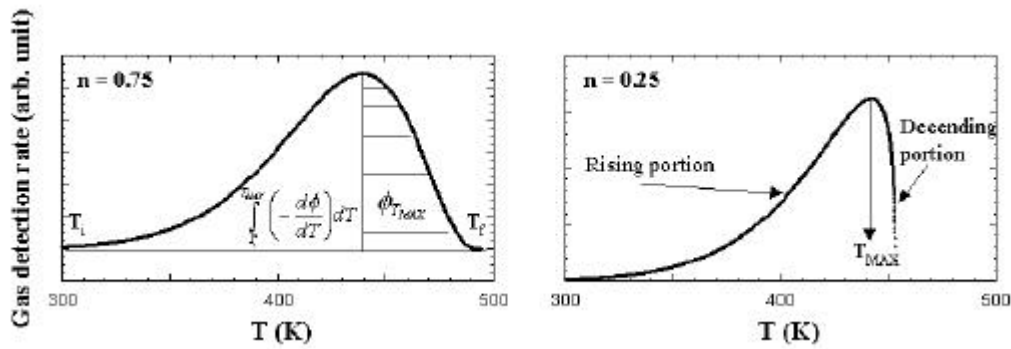


Fig. 1: Simulations of the TPD/TPR curves with  $n = 0.75$  (left) and  $n = 0.25$  (right).

The following relation holds true for all  $n$ :

$$\int_{T_i}^{T_f} \left( -\frac{df}{dT} \right) dT - \int_{T_i}^{T_{MAX}} \left( -\frac{df}{dT} \right) dT = f_{T_{MAX}} \quad (13)$$

where  $f_{T_{MAX}}$  represents  $f$  at  $T_{MAX}$  (illustrated in Fig. 1),  $T_i$  and  $T_f$  are  $T$  at the onset and at the end of the single TPR curve.

From the above figures, it is also observed that TPR curves of very different values of  $n$  have distinct shapes.

So for a given kinetic reaction order  $n$ :

$$\frac{f_{T_{MAX}}}{\int_{T_i}^{T_{MAX}} \left( -\frac{df}{dT} \right) dT} \approx b \quad (14)$$

where b is some constant.

The following table gives values of b for some values of n:

	<b>n = 0</b>	<b>n = 0.14</b>	<b>n = 0.25</b>	<b>n = 0.50</b>	<b>n = 0.75</b>	<b>n = 1.0</b>	<b>n = 1.5</b>	<b>n = 2.0</b>
<b>b</b>	0	0.13	0.22	0.40	0.56	0.70	1.02	1.24

*Table I: Values of b for some values of n.*

The empirical kinetic reaction order n can be obtained with the help of table I, or curve fitting with equations (9) or (10).

### **Determination of the activation energy E and pre-exponential factor v**

#### I/ VARIABLE LINEAR RAMP TECHNIQUE:

If the TPD/TPR peaks are not too broad and one can vary the ramp rate by 2 orders of magnitude, the analysis of this technique is straightforward and is recommended. The detailed analysis of this technique has been reported in a previous publication.<sup>7</sup>

#### II/ ARRHENIUS PLOT:

This technique is inherently very sensitive to small error in background subtraction.<sup>7</sup>

However, it offers a proper alternative way to obtain E and v if used carefully.

Taking the natural logarithm on both sides of the equation (8) yields:

$$\ln\left(-\frac{df}{dT}\right) = -\frac{E}{RT} + \ln\left(\left[\frac{u}{b}\right][f]^n\right) \quad (15)$$

Near the onset of the TPD/TPR curve:  $f \approx 1$  and equation (15) can be rewritten as:

$$\ln\left(-\frac{df}{dT}\right) \approx -\frac{E}{RT} + \ln\left(\frac{u}{b}\right) \quad (16)$$

If one fit a linear line through the Arrhenius plot of the natural logarithm of the TPD/TPR data vs.  $1/T$  near the onset of the TPD/TPR curve,  $E$  and  $v$  can be determined from the slope and the intercept of the linear fit.

### III/ ITERATIVE REGRESSION ANALYSIS:

Experimental TPD/TPR data can be fitted directly to equations (9) and/or (10) to obtain  $E$ ,  $v$ .<sup>7</sup> If the TPR curve is simple and does not require decomposition,  $n$  can be obtained most conveniently with a table similar to table I.  $E$  and/or  $v$  obtained from other techniques such as Arrhenius plot can be used as the starting point for the curve fitting process. Since in the Iterative Regression Analysis technique, data from the whole TPD/TPR curves are used instead of a small selected portion of data near the onset (Arrhenius plot) or at the local extrema (variable linear ramp) of the TPD/TPR curves, better accuracy in the results is expected. Fitting equations (9) and/or (10) to the whole set of TPD/TPR data curve is essentially solving a set of overdetermined equations (more independent equations than the unknowns to be determined). Note that since  $f$  in equation (8) is unitless, the unit of  $v$  is always  $s^{-1}$ , regardless of value of  $n$ . For a complex TPD/TPR curve that require decomposition, values of  $n$  and/or  $E$  or  $v$  that are given or obtained from other techniques/experiments for the leading or trailing decomposed curves are useful starting point for the curve fitting process.

### **Prediction of the decomposition of LiOH vs. time at constant temperature**

From equation (8):

For n=1:

$$-\frac{df}{f} = ue^{-\frac{E}{RT}} dt \quad (17)$$

or

$$\ln f = -\left(ue^{-\frac{E}{RT}}\right)t \quad (18)$$

or

$$f(t) = e^{-\left(ue^{-\frac{E}{RT}}\right)t} \quad (19)$$

For n = 2:

$$-\frac{df}{f^2} = ue^{-\frac{E}{RT}} dt \quad (20)$$

or

$$f(t) = \frac{1}{\left(ue^{-\frac{E}{RT}}\right)t + 1} \quad (21)$$

For n < 1:

$$-\frac{df}{f^n} = ue^{-\frac{E}{RT}} dt \quad (22)$$

or

$$f(t) = \left[ \frac{1}{(n-1)} \left\{ \frac{1}{\left( u e^{-\frac{E}{RT}} \right) t + \frac{1}{(n-1)}} \right\} \right]^{\frac{1}{(n-1)}} \quad (23)$$

## IV. RESULTS & DISCUSSION

### TPR of LiOH powders

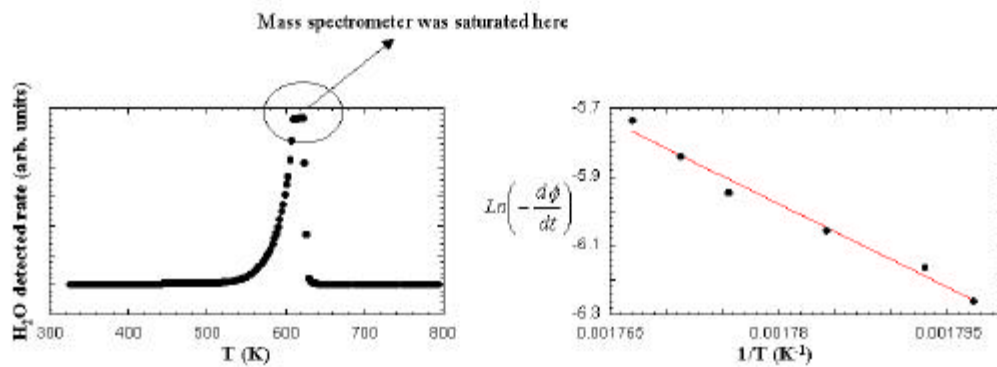


Fig. 2: The H<sub>2</sub>O TPR signal from LiOH powders and the corresponding Arrhenius plot near the TPR onset.

Fig. 2 shows the H<sub>2</sub>O TPR signals from LiOH powders and the corresponding Arrhenius plot near the TPR onset. There was only one decomposition energy site at around 620 K. Unfortunately, due to the saturation of the mass spectrometer signals near the peak of the LiOH decomposition TPR curve, the iteration regression analysis, which depends on the whole shape of the TPD/TPR curve, is not as accurate as the technique based on the Arrhenius plot near the onset of the TPR in obtaining activation energies. The activation energy of decomposition of LiOH is determined by plotting  $\ln[-df/dT]$  vs.  $1/T$  near the TPR onset to be in the range of 30 kcal/mol to 32.2 kcal/mol. The pre-exponential factor

is on the order of  $9.0 \times 10^8 \text{ s}^{-1}$  to  $8.5 \times 10^9 \text{ s}^{-1}$ . Based on equation (14) and the accompanying table, the kinetic reaction order  $n$  is between 0.5 and 0.75. The fact that the kinetic reaction order  $n$  for the LiOH decomposition process is not 2 suggests that the reaction  $2\text{LiOH} \Rightarrow \text{Li}_2\text{O} + \text{H}_2\text{O}$  in LiOH powders is not an elementary process. With an activation energy for the decomposition of 30 to 32 kcal/mol and a pre-exponential factor on the order of  $9.0 \times 10^8 \text{ s}^{-1}$  to  $8.5 \times 10^9 \text{ s}^{-1}$ , LiOH is very stable at room temperature. Fig. 3 shows the decomposition simulation curves for LiOH powders using the kinetic parameters obtained above in equation (23). It is seen from this figure that the decomposition of LiOH into  $\text{Li}_2\text{O}$  and  $\text{H}_2\text{O}$  is minimal even at 320 K over 100 years.

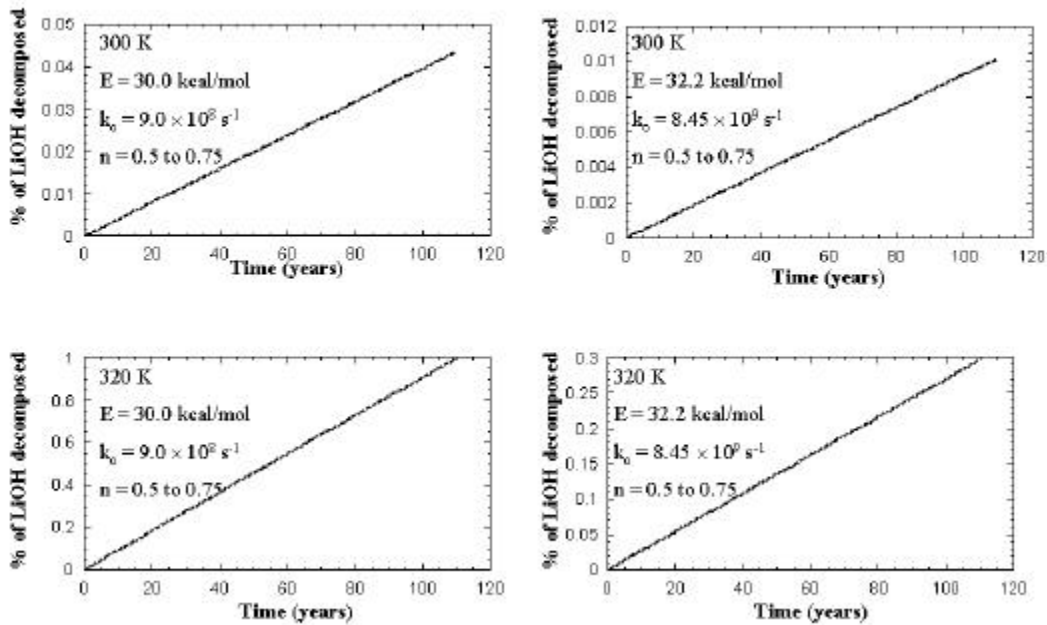
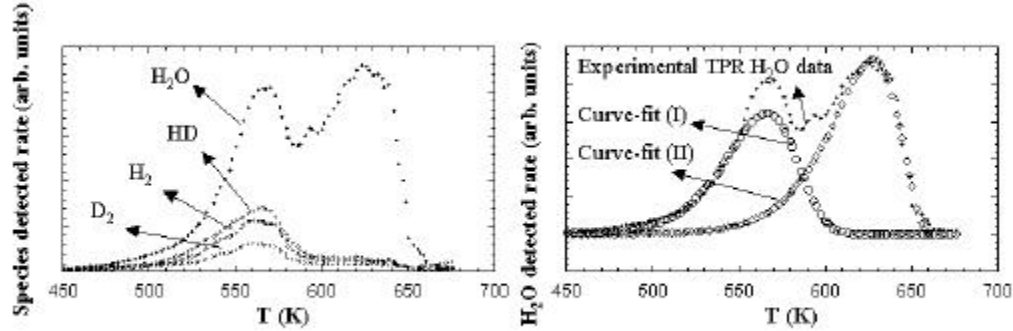


Fig. 3: Prediction of the decomposition of LiOH into  $\text{Li}_2\text{O}$  and  $\text{H}_2\text{O}$  at 300 K and 320 K over 100 years.

**TPR of a LiD single crystal previously exposed to air for 2 hours at approximately 30% to 40% relative humidity**



*Fig. 4: TPR data from a single crystal LiD previously exposed ambient air for 2 hours .*

Fig. 4 shows the TPR spectra of a LiD single crystal previously exposed to ambient air for 2 hours. Unfortunately, due to experimental difficulty with the heating system below 450 K, only data in the 450K to 700 K is presented here. The TPR data reveal that the decomposition of LiOH into Li<sub>2</sub>O and H<sub>2</sub>O has multiple activation energy barriers between 450 K to 700 K. The fitting of the H<sub>2</sub>O detected rate to equations (9) and (10) yields two separate decomposition curves: (I)  $n \approx 1$ ,  $E = 26$  to  $29.7$  kcal/mol,  $\nu = 1.53 \times 10^8$  to  $5.95 \times 10^9$  s<sup>-1</sup> and (II)  $n \approx 0.75$ ,  $E = 30.5$  to  $33.1$  kcal/mol,  $\nu = 7.72 \times 10^8$  to  $6.41 \times 10^9$  s<sup>-1</sup>. The decomposition curve (I) has a smaller activation energy barrier and is attributed to the decomposition of LiOH structures with a lot of defects such as dangling bonds, cracks, and other long range disorders. The decomposition curve (II) has a higher activation energy barrier and is attributed to the decomposition of LiOH structures with less defects. This is similar to the case of SiO<sub>2</sub> and SiO<sub>x</sub> with  $x < 1$ . In many cases, SiO<sub>x</sub> was found to be a network of SiO<sub>2</sub> with a lot of defects such as oxygen vacancies and broken or

dangling bonds.<sup>9</sup> Thermodynamically,  $\text{SiO}_x$  is not stable and will convert to  $\text{SiO}_2$ , but kinetically this may take a long time at room temperature. This is the reason why oxide grown on the surface of a Si wafer still has  $x < 2$  after many years of air exposure. This oxide can be removed by simply flash-heating the Si wafer in a vacuum to around 1000 C while true  $\text{SiO}_2$  films are stable even at much higher temperatures.<sup>10</sup> It is noted from Fig. 4 that the amounts of HD,  $\text{H}_2$ , and  $\text{D}_2$  detected were only a fraction of the amount of  $\text{H}_2\text{O}$  detected. They also evolved most heavily near the region of decomposition dominated by LiOH structures with more defects. This suggests that there are more defects in the LiOH structure near the LiD/ $\text{Li}_2\text{O}$ /LiOH interface where stress due to lattice mismatches is most pronounced. With a smaller activation energy barrier, LiOH structures with a lot of defects may decompose significantly over the next 100 years of storage at 320 K. Fig. 5 shows the simulated decomposition of two LiOH structures: one with less defects (30.5 kcal/mol) and one with more defects (26 kcal/mol) at 300 K and 320 K. As in the case of LiOH powders, the LiOH structure with  $E = 30.5$  kcal/mol decomposes minimally over 100 years. However, about 60 % of the defective LiOH structure with  $E = 26$  kcal/mol decomposes in the same time span at 320 K.

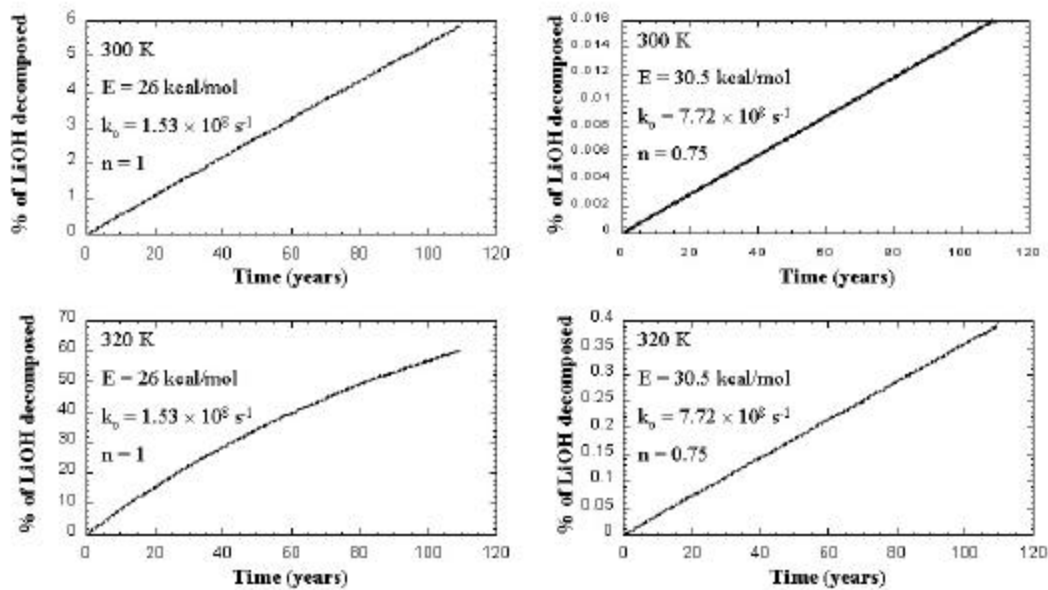
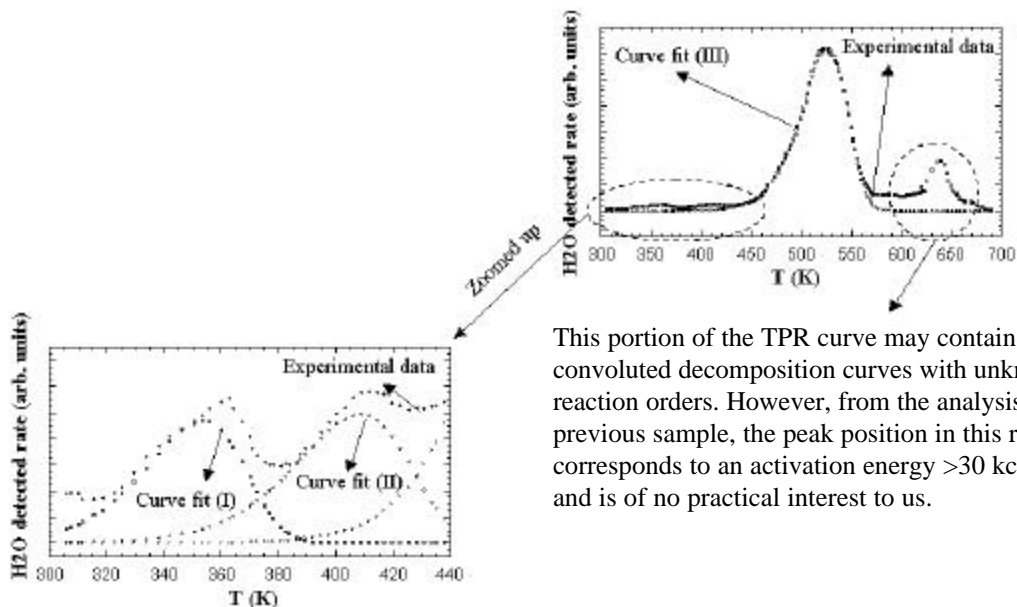


Fig. 5: Simulations of the decomposition of two LiOH structures: one with less defects (30.5 kcal/mol) and one with more defects (26 kcal/mol) at 300 K and 320 K.

**TPR of a LiD single crystal previously exposed to ambient air for 8 minutes at an approximately 30% to 40 % relative humidity.**

Fig. 6 shows the TPR curve of another LiD single crystal previously exposed to ambient air for 8 minutes. This sample was pumped for a few hours following the moisture exposure step and before the TPR experiment.



This portion of the TPR curve may contain up to 4 convoluted decomposition curves with unknown reaction orders. However, from the analysis of the previous sample, the peak position in this region corresponds to an activation energy  $>30$  kcal/mol and is of no practical interest to us.

Fig. 6:  $H_2O$  TPR signal from a LiD single crystal previously exposed to air for 8 minutes.

Using equations (9) and (10), the first 3 peaks in the TPR curve for this sample can be fitted with:

- Curve fit (I):  $n = 1$ ,  $E = 13.8$  to  $14.6$  kcal/mol,  $\nu = 7.45 \times 10^6$  to  $2.43 \times 10^7$   $s^{-1}$
- Curve fit (II):  $n = 1$ ,  $E = 14.9$  to  $16.0$  kcal/mol,  $\nu = 1.96 \times 10^6$  to  $7.47 \times 10^6$   $s^{-1}$
- Curve fit (III):  $n = 1$ ,  $E = 22.5$  to  $22.9$  kcal/mol,  $\nu = 3.87 \times 10^7$  to  $5.69 \times 10^7$   $s^{-1}$

The  $H_2O$  peaks corresponding to curve fits (I) and (II) have activation energies less than 16 kcal/mol and can be best attributed to water molecules in the  $LiOH \cdot H_2O$  structure formed during 8 minutes exposure to moisture at 50 % relative humidity prior to TPR experiment. The  $H_2O$  peak corresponding to curve fit (III) with  $E = 22.5$  to  $22.9$  kcal/mol is attributed to the decomposition of  $LiOH$  with a lot of defects. The portion of the TPR curve after this peak may contain up to 4 convoluted decomposition curves with unknown reaction orders. However, from the analysis of the previous sample, the peak position in

this region corresponds to an activation energy  $>30$  kcal/mol. This peak is stable and provides no practical interest. By comparing the TPR curves obtained from the sample previously exposed to air for 2 hours and the one previously exposed to air for 8 minutes, the LiOH films formed on different LiD samples may not have the same structural integrity, and hence exhibit slightly different TPR decomposition behaviors.

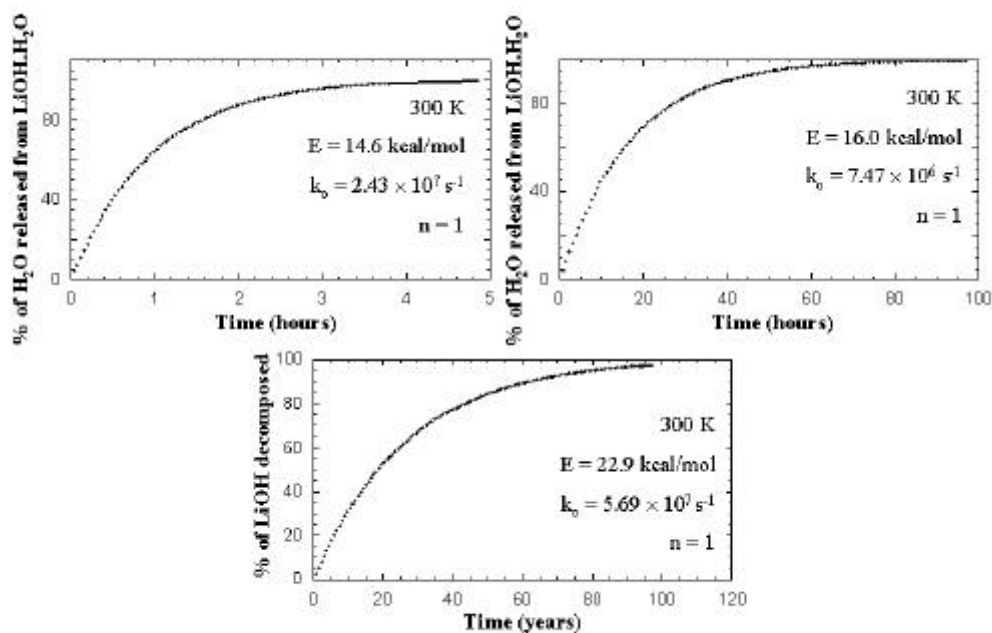


Fig. 7: The simulated release of H<sub>2</sub>O from LiOH.H<sub>2</sub>O structures and the decomposition of LiOH structure with E = 22.9 kcal/mol at room temperature.

Fig. 7 shows the simulated release of H<sub>2</sub>O from LiOH.H<sub>2</sub>O structures and the decomposition of LiOH structure with E = 22.9 kcal/mol at room temperature. It can be seen from the figure that H<sub>2</sub>O molecules from LiOH.H<sub>2</sub>O structures can be effectively pumped away at room temperature. Seventy two hours of pumping at room temperature is enough to remove essentially all H<sub>2</sub>O from the LiOH.H<sub>2</sub>O structures. However, highly defective LiOH, which may not be significantly pumped away even at 350 K in a

reasonable time (days to weeks), may severely decompose in the next 100 years. For example, at 300 K, almost 100 % of defective LiOH structures with an activation energy of  $E = 22.9$  kcal/mol and a pre-exponential factor  $\nu = 5.69 \times 10^7$  s<sup>-1</sup> will decompose in the next 100 years.

**TPR of LiD which had been annealed to 503 K for 48 hours, cooled down to room temperature, then exposed to different dosages of H<sub>2</sub>O**

In this set of experiments, a LiD single crystal, which had been annealed to 503 K for 48 hours in an ultrahigh vacuum environment and then cooled down to room temperature, was exposed to 39 ppm of moisture for 4 hours prior to TPD experiment. After that, the same sample was subjected to the same heating and cooling cycle described above, then exposed to 399 ppm of moisture for 3.2 hours prior to TPD experiment. A similar heating and cooling cycle was applied to the sample before it was exposed once again to moisture at 779 ppm for 20 hours. The upper part of Fig. 8 shows the TPR spectra of this sample after three separate moisture exposures. It is noted that as the level of water exposure increased, the first TPR peak shifted to higher temperature, implying an increase in the activation energy of decomposition of LiOH. Since these TPR spectra consist of many heavily convoluted decomposition curves, the kinetic reaction orders of which are not known in the temperature range of 300 K to 570 K, the application of the iterative regression analysis to extract kinetic parameters from the spectra is not practically suitable. In order to successfully employ the technique of iterative regression analysis for heavily convoluted TPD/TPR spectra, information on the kinetic reaction order  $n$  for the decomposition curve at either the trailing or leading edge is needed. However, without deconvoluting the spectra, the activation energy of reaction for the component with lowest

activation energy for each TPR curve in Fig. 8 can still be obtained from the Arrhenius plot based on equation (15).

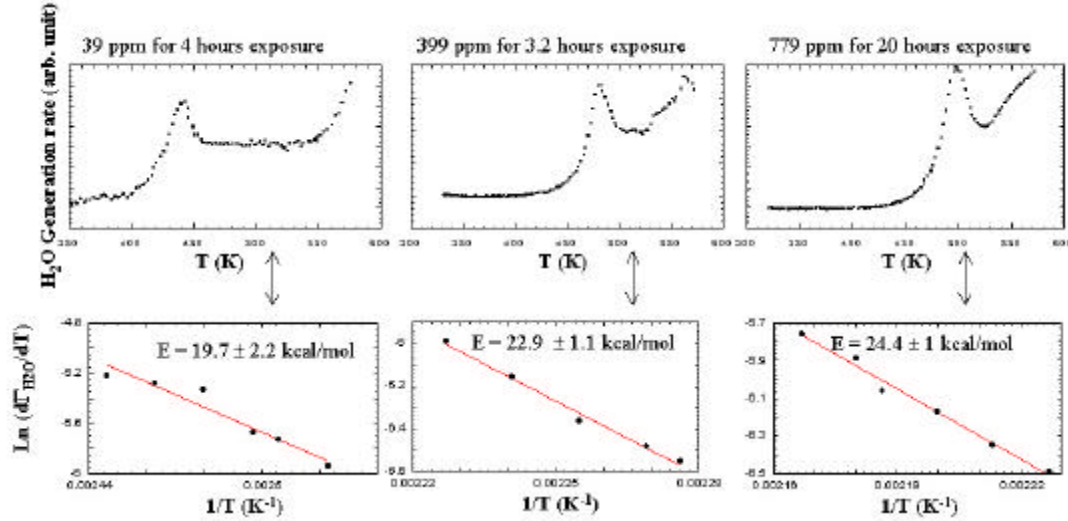


Fig. 8: H<sub>2</sub>O TPR spectra of a LiD single crystals, which had been heat treated to 503 K for 48 hours and then cooled down to room temperature, after three separate moisture exposures and the corresponding Arrhenius plots for the determination of the activation energy of decomposition in the three cases.

In the lower part of Fig. 8, we show the Arrhenius plot for the determination of the activation energy of decomposition in the three cases. It is seen, here, that the lower levels of moisture exposure formed "poor quality" LiOH which decomposed at lower temperatures than the "good quality" LiOH formed at higher levels of moisture exposure. In the Arrhenius plots,  $\Gamma_{\text{H}_2\text{O}}$  designates the flux of H<sub>2</sub>O detected by the mass-spectrometer. So, in general, we observe that at lower exposure dosages, the LiOH formation is highly defective and has components which tend to decompose at much lower activation energy barrier than 30 kcal/mol.

In Fig. 9, we show qualitatively the different growth paths for LiOH on LiD single crystals as a function of moisture exposure.

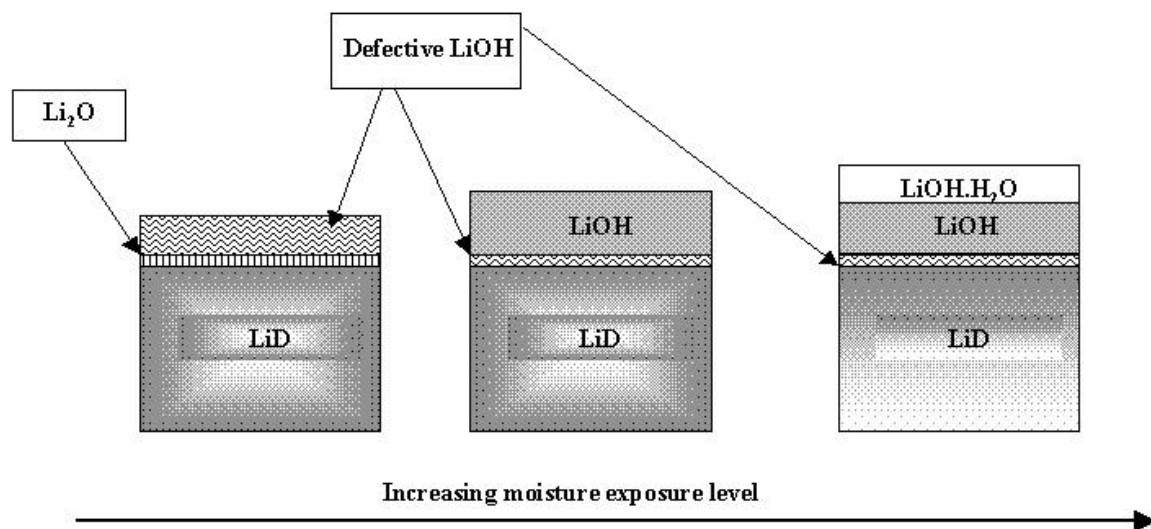


Fig. 9: Growth paths for LiOH on LiD as a function of moisture exposure levels

It is seen from this figure that as a result of long exposure in a moist environment, one can grow stoichiometric and good quality LiOH.H<sub>2</sub>O or LiOH on LiD single crystals. There would always be some defective LiOH structures near the LiOH/LiD interface, however, due to lattice mismatch induced stress there. In a dry environment with residue moisture on the order of a few ppm, LiOH structures with dangling bonds, cracks, and other long range disorders are predominant, even far away from the LiOH/Li<sub>2</sub>O/LiD interface. Note that in a vacuum or dry environment, due to a lack of supply of H<sub>2</sub>O molecules to the LiOH/LiD interface, LiD reacts with LiOH to form Li<sub>2</sub>O and hydrogen species instantaneously at the interface and hence the formation of LiD/Li<sub>2</sub>O/LiOH interface.

### **The reaction of LiD with moisture at elevated temperatures**

Fig. 10 shows that the reaction of LiD with moisture is significantly reduced at elevated temperatures, even at atmospheric pressures with 50 % relative humidity. From the figure, it is seen that at 50 % relative humidity, air exposure of the LiD single crystal labeled

“Sample 1a” for 30 hours at  $T = 300\text{ K}$  resulted in  $\sim 30\text{ }\mu\text{m}$  thick of reacted layer (LiOH and/or  $\text{LiOH}\cdot\text{H}_2\text{O}$ ). “Sample 1a” and “Sample 1b” were originally from the same LiD single crystal which was subsequently cleaved into two smaller pieces. “Sample 1b” was subjected to the same moisture exposure conditions as “Sample 1a”, except at a slightly elevated temperature of  $T = 339\text{ K}$ . The reacted layer from “Sample 1b” was less than  $6\text{ }\mu\text{m}$ .

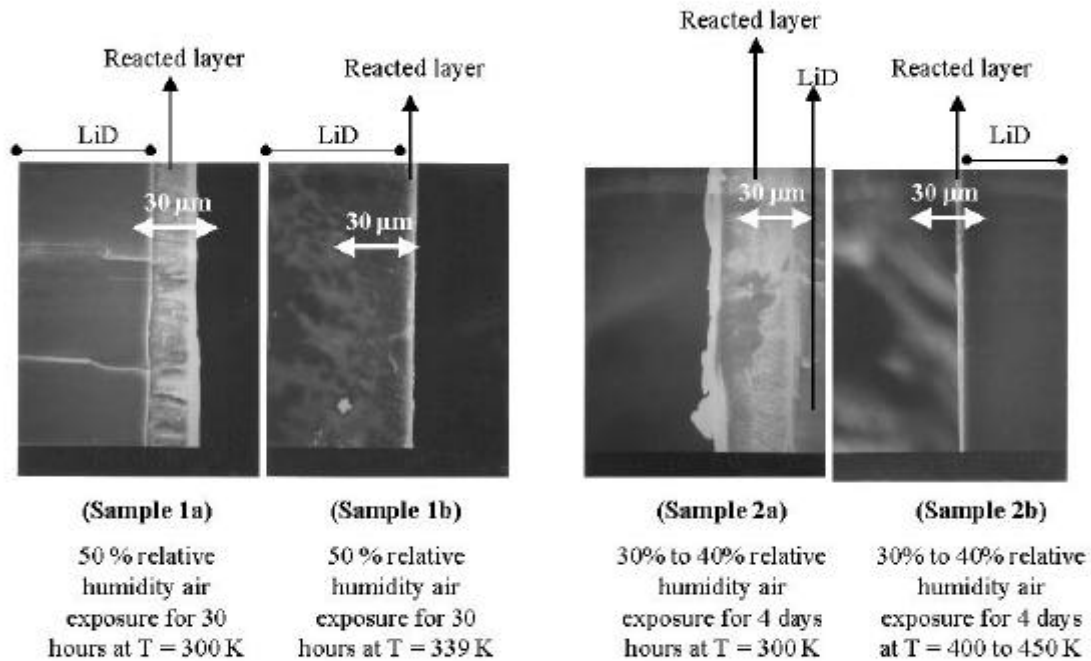


Fig. 10: SEM shows that the reaction of LiD with moisture is greatly reduced at elevated temperatures.

On a different day, another LiD single crystal was cleaved into two halves labeled "Sample 2a" and "Sample 2b". "Sample 2a" was exposed to ambient air at 30% to 40% relative humidity for 4 days at  $T = 300\text{ K}$  while "Sample 2b" was exposed to the same ambient environment for 4 days at a temperature between  $400\text{ K}$  and  $450\text{ K}$ . The reacted

layer thickness on "Sample 2a" was more than 30  $\mu\text{m}$  while that of "Sample 2b" was only about 4 to 5  $\mu\text{m}$ . We attribute the much more reduced reaction rate of LiD with moisture at elevated temperatures to the reduced sticking probability of  $\text{H}_2\text{O}$  molecules on a hot surface.

#### **IV. CONCLUSION & DISCUSSION**

We have performed TPR on LiOH powders and LiD single crystals previously exposed to different moisture levels. Our results show that the decomposition process of LiOH has a high activation energy barrier of between 30 kcal/mol and 33.1 kcal/mol. The LiOH structure is stable even if kept at an elevated temperature of 320 K for 100 years. However, LiOH structures formed at low levels of moisture exposure may have an activation energy barrier much lower than 30 kcal/mol. This activation energy barrier decreases with decreasing moisture exposure level. We attribute the low activation energy barriers for the decomposition of these LiOH structures formed at low levels of moisture exposure to the existence of dangling bonds, cracks, and other long range disorders in the LiOH structures. These defective LiOH structures may decompose significantly over the next 100 years of storage even at room temperature. At very high moisture exposure levels, the release of  $\text{H}_2\text{O}$  molecules from  $\text{LiOH}\cdot\text{H}_2\text{O}$  structure has a small activation energy barrier of between 13.8 kcal/mol to 16.0 kcal/mol. The loosely bonded  $\text{H}_2\text{O}$  molecules can be easily pumped away at room temperature in a reasonable amount of time. We are actively doing experiments on  $\text{Li}_2\text{O}$  powders to determine the reaction probability of  $\text{Li}_2\text{O}$  with  $\text{H}_2\text{O}$  to reform LiOH and to quantify the ratios of bad quality LiOH over good quality LiOH under a variety of moisture exposure levels. We also

intend to obtain a well calibrated four dimensional plot of the reaction probability of LiD and Li<sub>2</sub>O with moisture as a function of moisture pressure, time, and temperature. Finally, our experiments suggests that handling LiD at an elevated temperature of 340 K or more efficiently reduces the growth of LiOH and LiOH.H<sub>2</sub>O. Therefore, a proposed way of minimizing hydrogen formation (due to H<sub>2</sub>O reaction with LiD) in a closed system containing LiOH in the presence of LiD is to handle LiD at an elevated temperature whenever possible (during transportation prior to heat-treatment as well as during assembly).

## **V. ACKNOWLEDGEMENT**

This work was performed under the auspices of the U.S. Department of Energy by Lawrence Livermore National Laboratory under contract No. W-7405-ENG-48.

## **REFERENCES**

1. S. M. Myers, Ion-backscattering study of LiOH-to-Li<sub>2</sub>O conversion on a LiH substrate, *Journal of Applied Physics*, **45**, 4320, (1974).
2. J. Philips and A. Graham, Investigation of Lithium Compound Reactions with Water, Oxygen and Carbon Dioxide, unpublished, (1999).
3. L. N. Dinh, M. Balooch, J. D. LeMay, Desorption kinetics of H<sub>2</sub>O, H<sub>2</sub>, CO, and CO<sub>2</sub> from silica reinforced polysiloxane, UCRL-ID-135387, Lawrence Livermore National Laboratory (1999).
4. D. Perez-Bendito and M. Silva, *Kinetic Methods in Analytical Chemistry*, Halsted Press, New York (1988).
5. G. Pannetier and P. Souchay, *Chemical Kinetic*, Elsevier, Amsterdam-New York (1967).
6. F. Acke, I. Panas, *Thermochemica Acta* **306**, 73 (1997).
7. K. H. Van Heek and H. Juntgen, *Berichte Der Deutschen Bunsengesellschaft Fur Physikalische Chemie*, vol. **72**, 1223(1968).
8. L. N. Dinh, M. Balooch, J. D. LeMay, UCRL-ID-137614, Lawrence Livermore National Laboratory (2000).
9. L. N. Dinh, L. L. Chase, M. Balooch, F. Wooten, W. J. Siekhaus, Optical properties of passivated Si nanocrystals and SiO<sub>x</sub> nanostructures, *Phys. Rev. B* **54**, 5029 (1996).
10. L. N. Dinh, M. Balooch, unpublished.